Selected Papers

Chemistry of Anthracene–Acetylene Oligomers. XVIII. Construction and Structures of Belt-Shaped Macrocyclic Oligomers with Anthracene Units and Acetylene Linkers and Resolution of Chiral Derivatives[1]

Takeharu Ishikawa,[1] Tetsuo Iwanaga,[1] Shinji Toyota,*[1] and Mikio Yamasaki[2]

[1]Department of Chemistry, Faculty of Science, Okayama University of Science, 1-1 Ridaicho, Kita-ku, Okayama 700-0005

[2]Rigaku Corporation, 3-9-12 Matsubaracho, Akishima, Tokyo 196-8666

Received February 28, 2011; E-mail: stoyo@chem.ous.ac.jp

Acyclic anthracene–acetylene trimers consisting of two 1,8-anthrylene units and one 1,5- or 1,8-anthrylene unit were cyclized by Eglinton coupling to form the corresponding cyclic trimer, hexamer, and higher oligomers. The molecular structures of these oligomers were investigated by X-ray analysis and DFT calculations at the M05/3-21G level. The trimers have rigid macrocyclic frameworks and the hexamer and higher oligomers prefer to take flat or folded structures due to transannular $\pi\cdots\pi$ interactions between the anthracene units. Cyclic hexamers and higher oligomers feature chiral structures that are likened to figure-eight or directional belts. The enantiomers of some chiral cyclic oligomers were resolved by chiral HPLC. The dynamic behavior of the macrocyclic frameworks and each anthrylene unit was observed by variable-temperature ^{1}H NMR measurements. The electronic spectra of these cyclic oligomers are discussed in terms of ring size and the combination of anthrylene units.

In our series of studies on anthracene–acetylene oligomers, we have synthesized several cyclic oligomers having interesting structures and properties. Some examples are 1,8-anthrylene–ethynylene cyclic tetramers **1** and hexamers **2** in Figure 1 (hereafter, *n*-mer refers to an oligomer with *n* anthracene units regardless of the position of substitution and the kind of linker).[1,2] Recently, we reported chiral cyclic compound **3a** consisting of four anthracene units and four acetylene linkers, and successfully resolved its enantiomers by chiral HPLC without racemization via rotation of the 1,5-anthrylene units (1,5-A, *x*,*y*-substituted anthracene is abbreviated as *x*,*y*-A hereafter) about the linker moieties.[3] For the synthesis of **3a**, we needed to prepare acyclic trimer **4a** as its precursor. We thought that this precursor **4** and its 1,5-A analog **5** would give novel cyclic frameworks $\mathbf{6}_n$ and $\mathbf{7}_n$, respectively. While their intramolecular cyclization should lead to strained cyclic trimers ($\mathbf{6}_1$ and $\mathbf{7}_1$), their oligomerization followed by cyclization should lead to larger macrocyclic compounds [$\mathbf{6}_n$ and $\mathbf{7}_n$ ($n \geq 2$)]. According to the geometric requirement suggested by molecular models, these higher oligomers are expected to form belt-shaped structures that are chiral; the chirality is due to the presence of wave-like directional links along the belt surface, in contrast to achiral 1,8-A cyclic hexamer **2b** ($x = 1$).[1] Hexamers $\mathbf{6}_2$ and $\mathbf{7}_2$ are also regarded as figure-eight molecules of chiral D_2 symmetry. In π-conjugated macrocyclic compounds, belt-like or figure-eight-shaped motifs are attractive because they can be used to realize unique properties and topologies.[4] Expanded porphyrins have been extensively studied as helical and figure-eight-like macrocycles[5] and circulenes with such structures are still target compounds of synthetic interest.[6] Typical examples of molecular belts are cyclacene derivatives, arylene–ethynylene oligomers, and cyclo-*p*-phenylenes.[4,7,8] As regards chiral cyclic oligomers, several anthrylene oligomers **1b**, **2b** ($x = 2$), and **3a**[1,3,9] as well as a substituted picotube[10] were successfully resolved by chiral HPLC. These enantiopure samples gave valuable information on the chiroptical properties of chiral π-conjugated macrocyclic compounds because the resolution of such aromatic hydrocarbons is generally difficult. We also applied this methodology to chiral cyclic oligomers $\mathbf{6}_n$ ($n = 2$) and $\mathbf{7}_n$ ($n = 2$, 3, and 4) to obtain conclusive evidence of chiral structures. We herein report the synthesis, structures, and dynamic behavior of these macrocyclic compounds and the chiroptical properties of the chiral analogs.

Results and Discussion

Synthesis and Characterization. The target compounds were synthesized according to the reactions shown in Scheme 1. As for cyclic oligomers $\mathbf{6}_n$, we prepared not only butyl derivatives but also octyl derivatives because the very low solubility of $\mathbf{6a}_2$ obstructed its purification and spectroscopic measurements. Trimers **4a** and **4b** were prepared by the Sonogashira coupling of corresponding alkynes **8**[1,2] and 9,10-diiodoanthracene (**9**)[11] in a 2:1 ratio. Trimer **5a** with a 1,5-A unit was similarly prepared from **8a** and 1,5-diiodoanthracene (**10**).[12] Precursor **4b** was desilylated with tetrabutylammonium fluoride (TBAF) in THF and the formed terminal alkyne was subjected to Eglinton coupling[13] without purification in

Published on the web June 18, 2011; doi:10.1246/bcsj.20110066

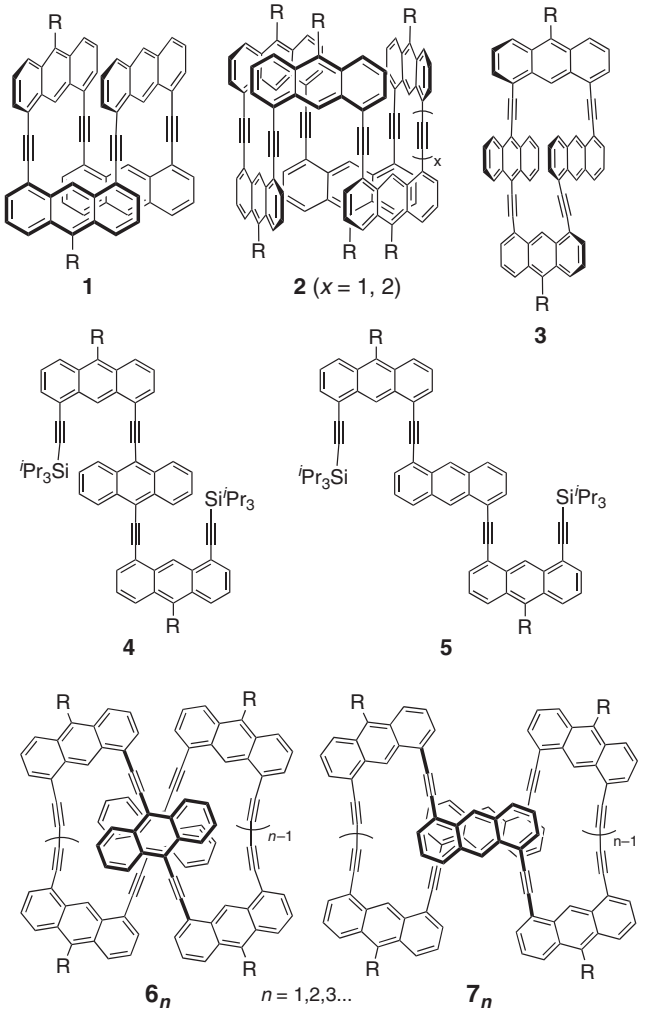

Figure 1. Anthrylene–ethynylene oligomers.

1 mmol L^{-1} pyridine solution. The products were separated by chromatography on silica gel and then GPC to give trimer **6b$_1$** and hexamer **6b$_2$** in 40 and 32% yields, respectively. The reaction with **4a** gave **6a$_1$** and **6a$_2$** in 37 and 20% yields, respectively. Macrocyclization of **5a** was similarly carried out. The crude products were purified by chromatography on silica gel to afford a small amount of pure **7a$_1$** that was very poorly soluble and a mixture of other oligomers. The latter was further purified by GPC to give hexamer **7a$_2$** (30%), nonamer **7a$_3$** (15%), and dodecamer **7a$_4$** (14%). The chromatogram showed the presence of higher oligomers, but we failed to separate them in the pure form. Those oligomers are yellow solids except for **6a$_2$** and **6b$_2$**, which are reddish due to absorption at longer wavelengths. The exact molecular weights of the trimers and the hexamers were confirmed by high-resolution FAB mass spectroscopy. The molecular ion peaks of nonamer **7a$_3$** and dodecamer **7a$_4$** observed by MALDI-TOF mass spectroscopy are consistent with the simulated isotope patterns.

The ^{1}H NMR spectra of the cyclic compounds are as simple as those of the acyclic precursors, reflecting symmetric structures on the NMR time scale. Compounds **6b$_1$** and **6b$_2$** gave two sets of the ABC system and one singlet due to 1,8-A units and one set of the AA′BB′ system due to 9,10-A units in the aromatic region. It is characteristic that the AA′BB′ signals of **6b$_2$** at δ 7.49 and 8.33 are broad at room temperature, and this observation will be discussed later in the section on dynamic behavior. Oligomers **7a$_n$** gave two sets of the ABC system and one singlet due to 1,8-A units and one set of the ABC system and one singlet due to 1,5-A units. While the signals due to H-9,10 in the 1,5-A units were observed at δ ca. 9.2 for acyclic trimer **5a** and cyclic trimer **7a$_1$**, the corresponding signals shifted upfield to δ 8.4 for higher cyclic oligomers **7a$_2$**–**7a$_4$**. This difference can be explained by the molecular structures, as mentioned below. The ^{13}C NMR spectra of **6b$_1$** and **6b$_2$** gave four alkyne signals at similar chemical shifts: for example, δ 81.1 and 85.1 due to the diacetylene carbons and δ 93.5 and 101.1 due to the acetylene carbons for **6b$_2$**. One of the diacetylene carbon signals at δ 85.1 unambiguously shifted downfield compared with those of the other cyclic oligomers, for example, the 1,8-A tetramer with four diacetylene linkers (δ 81).[9c] This effect is attributed to the bending deformation of alkyne carbons in the cyclic structures, as is generally observed for strained alkynes.[14] Hexamer **7a$_2$** also gave four alkyne carbon signals in the ^{13}C NMR spectrum, being consistent with the molecular structure. The chemical shifts of the diacetylene carbons, δ 79.4 and 82.5, appeared in the predicted region.

Electronic Spectra. The UV–vis and fluorescence spectra of **6b$_n$** and **7a$_n$** were measured in $CHCl_3$ (Figure 2). The spectroscopic data of the cyclic oligomers and their precursors are compiled in Table 1. The p-band absorptions of the oligomers with 1,5-A units (**7a$_n$**) were observed at 400–480 nm, and their intensities increased with ring size enlargement although they were not always additive. The peaks at the longest wavelength are almost independent of the ring size at 460 nm, and this wavelength is longer by ca. 30 nm than that of precursor **5a**. In contrast, the corresponding absorption peaks for the oligomers with 9,10-A units shifted to longer wavelength in the order of **4b** (443 nm), **6b$_1$** (491 nm), and **6b$_2$** (523 nm). These data are consistent with the fact that 9,10-diethynylanthracene chromophores produced a large bathochromic effect relative to other diethynylanthracenes,[2,15] and effectively extend the π-conjugation as observed for the *p*-phenylene–ethynylene system.[16]

In the fluorescence spectra of **7a$_n$**, broad emission bands were observed with peaks at 485–506 nm. The absolute fluorescence quantum yield of the dodecamer ($\Phi_f = 0.14$) is apparently smaller than those of the other cyclic oligomers ($\Phi_f = 0.41$–0.50). Fluorescence lifetime measurements revealed that only the dodecamer exhibited the emissions of two components at 1.4 and 3.5 ns, meaning the presence of contribution of the excimer-type emission. These phenomena are attributable to the intramolecular $\pi\cdots\pi$ interactions between anthracene moieties in the cyclic framework of **7a$_4$**.[17] As for oligomers **6b$_n$**, the emission peaks were observed at 541 and 564 nm for the cyclic trimer and the hexamer, respectively, showing a significant red shift upon ring size enlargement. The fluorescence quantum yields and lifetimes are comparable for the two compounds. The Stokes shifts are in the range of 22–77 nm for the acyclic and cyclic oligomers, and there is no clear tendency upon cyclization and ring size in the two series of compounds.

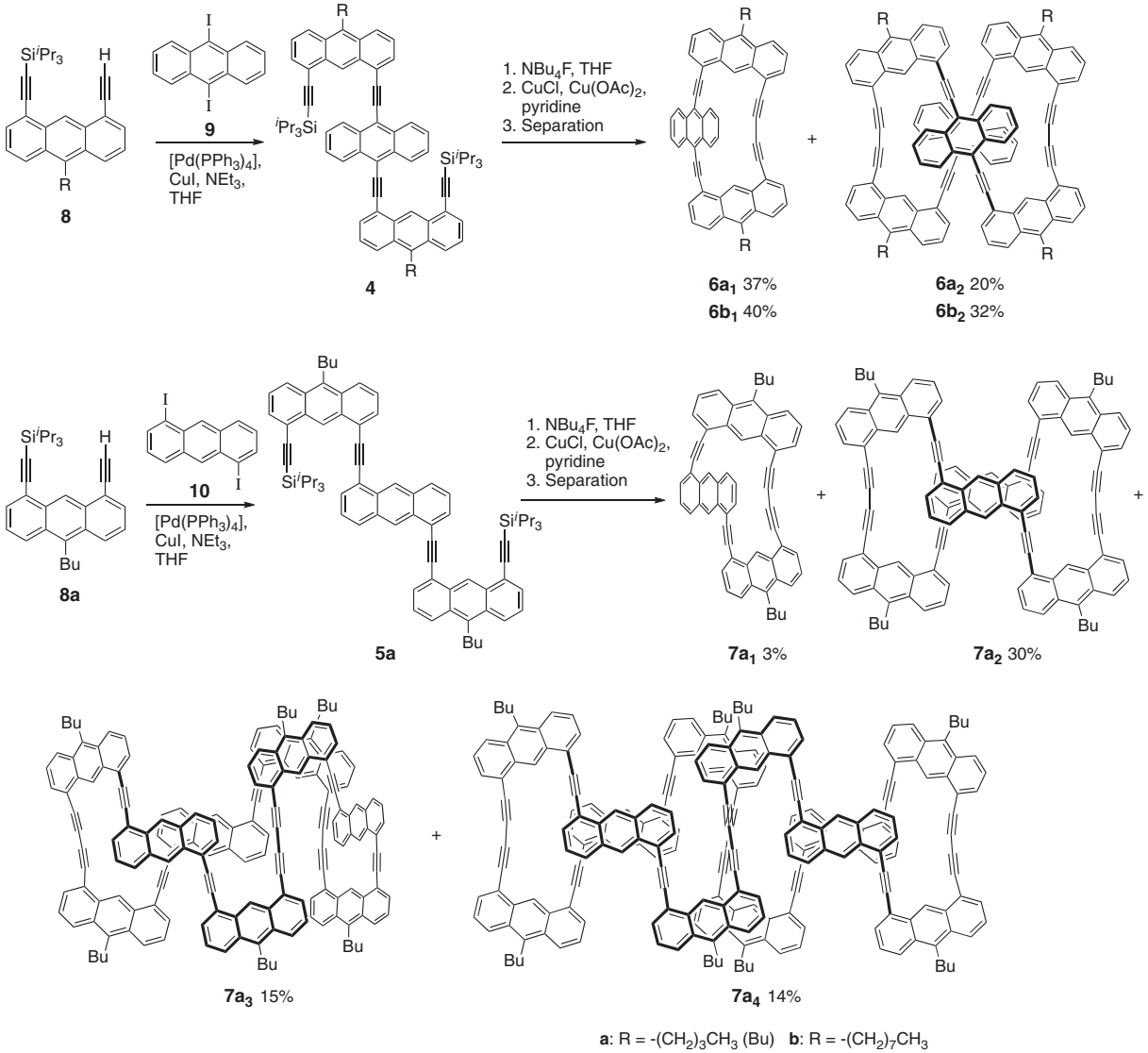

Scheme 1. Synthesis of cyclic oligomers $\mathbf{6}_n$ and $\mathbf{7}_n$.

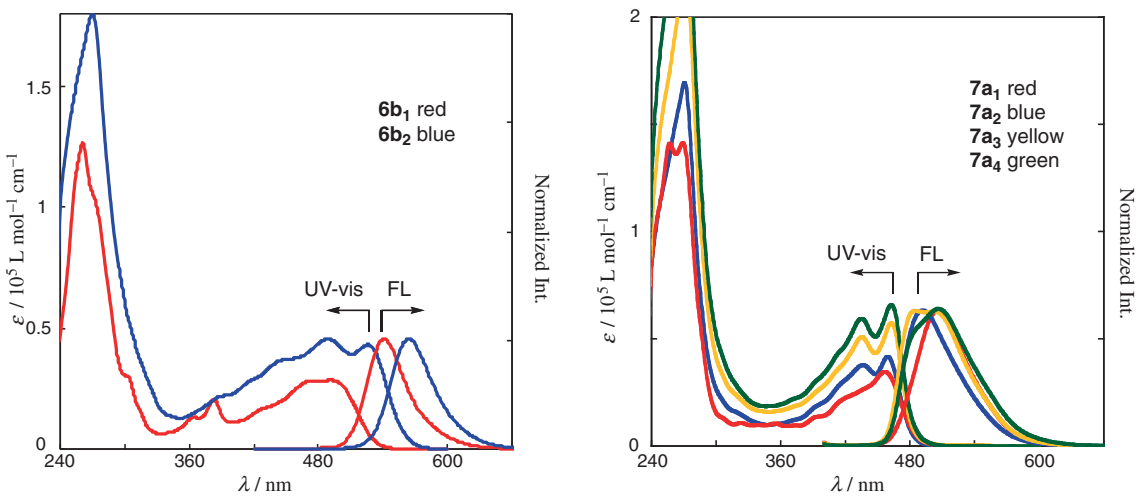

Figure 2. UV–vis and fluorescence spectra of $\mathbf{6b}_n$ and $\mathbf{7a}_n$ in $CHCl_3$.

Table 1. UV–vis and Fluorescence Spectral Data of Cyclic Oligomers and Their Acyclic Precursors in Chloroform

	UV	FL[b]			Stokes shift
	λ_{max}/nm (ε)[a]	λ_{max}/nm	Φ_f[c]	τ_f/ns[d]	/nm
4b	443 (34000)	520	0.82	2.7	77
6b$_1$	491 (28400)	541	0.68	3.5	50
6b$_2$	523 (33800)	564	0.69	4.5	41
5a	428 (30000)	458	0.64	2.7	30
7a$_1$	457 (34600)	506	0.50	2.7	49
7a$_2$	460 (41700)	494	0.49	3.7	34
7a$_3$	463 (57300)	485	0.41	3.5	22
7a$_4$	463 (65800)	506	0.14	1.4, 3.5	43

a) Wavelength and molar extinction coefficient of the peak at the longest wavelength in the p-band region. b) Excited at 393 nm. c) Absolute fluorescence quantum yield. d) Fluorescence lifetime.

Molecular Structures. X-ray analyses were carried out for **6a$_1$** and **7a$_1$**–**7a$_3$**, and their structures are shown in Figure 3. All single crystals include solvent molecules that are for clarity not shown in the structures except for hexane molecules in **7a$_3$**. The butyl groups in **6a$_1$** and **7a$_1$** are disordered in the crystals. An asymmetric unit of **7a$_1$** contains a half of the molecule, and the other half is symmetrically related.

In the structure of **6a$_1$**, the macrocyclic framework consisting of two 1,8-A units and the alkyne carbons are practically planar, and the 9,10-A plane is rotated by 45° from the coplanar conformation. The bond angles of the eight alkyne carbons are in the range of 167–173° and small angles are found at the two outer carbons in the diyne moiety. The structure of **7a$_1$** is chiral with a C_2 axis within a single molecule passing through the midpoint of the diyne linker and the centroid of a 1,5-A moiety. The dihedral angle between the two 1,8-A planes about the diyne linker is ca. 110° relative to the fully coplanar conformation, and the 1,5-A moiety shows small out-of-plane deformations around the 1,5-carbon atoms attached to the acetylene linkers. The closest distance between the diyne and the 1,5-A moiety is 3.84 Å, which is slightly longer than the sum of the van der Waals radii of unsaturated carbons (ca. 1.7 Å for each C).

Compound **7a$_2$** takes a flat structure of approximate C_2 symmetry, and a little twisted from the ideal D_2 symmetric structure. The two 1,5-A moieties, A1 and A4, are oriented in parallel at the interlayer distance of 3.53 Å, and they are tilted by 21° from each other. Among four 1,8-A moieties, A2 and A5 are nearly coplanar to the attached 1,5-A units and the others, A3 and A5, are significantly rotated from the coplanar conformation. Each alkyne carbon is not bent so much (bond angle 170–178°), but the diyne linkers are significantly curved to connect two 1,8-A moieties in a nonlinear fashion. The framework models of **7a$_3$** in Figure 3 show that the molecules are flat and slightly bent rather than expanded regardless of several degrees of freedom at the linker moieties. The preference for such conformation is attributable to the transannular $\pi\cdots\pi$ interactions, where there are two pairs of partially stacked anthracene groups (B1···B4 3.53 Å, B6···B9 3.62 Å) in addition to some close contacts between the anthracene and the triple bond moieties, particularly B7 at ca. 3.2 Å. It is interesting that one hexane molecule is included between the two anthracene moieties, B5 and B8, in the macrocyclic belt in the crystal. In other words, flexible belt-shaped molecules tend to reduce empty spaces by folding their frameworks and accommodating external molecules.

The structures of cyclic trimers, **6c$_1$** and **7c$_1$**, and hexamers, **6c$_2$** and **7c$_2$**, without alkyl groups were optimized by DFT calculations (Figure 4). We applied the M05 functional[18] and the 3-21G basis set because this level of calculations was found to reproduce the experimental structures of similar macrocyclic oligomers within an acceptable computation time.[1,3,9c] The observed structures of the macrocyclic frameworks of trimers were well reproduced by the calculations of **6c$_1$** and **7c$_1$**. One discrepancy is the conformation of the 9,10-A unit in **6c$_1$**, which is nearly perpendicular to the macrocyclic framework in contrast to the X-ray structure of **6a$_1$**. This linear anthracene unit can rotate readily within a range unless the steric hindrance by the macrocyclic framework becomes large. The calculation of **7c$_2$** gave a C_2 symmetric structure with close and parallel orientation of two 1,5-A units, the interlayer distance of which was 3.6 Å. This structural feature is in agreement with that of the X-ray structure of **7a$_2$**. The global minimum structure of **6c$_2$** is approximately C_2 symmetric, and two 9,10-A units are parallel at a distance of 3.5 Å and tilted by 60° with respect to each other. Unfortunately, we could not calculate the structures of the larger oligomers of **7c$_3$** and **7c$_4$** at this level because of limitations in computational performance.[19] These higher oligomers should prefer to take a folded conformation similar to the X-ray structure of **7a$_3$** in crystals. The shielding of H-9,10 atoms in the 1,5-A units of **7a$_2$**–**7a$_4$**, as mentioned above, is attributable to the ring current effect of the stacking anthracene moieties in the folded conformation.

Dynamic Behavior. Assuming that the cyclic oligomers are linkages, the degrees of freedom of the macrocyclic framework can be calculated with mechanical theory.[20] Trimers **6c$_1$** and **7c$_1$** have only one degree of freedom, the rotation of 9,10-A and 1,5-A moieties, respectively. Hexamer **6c$_2$** has three degrees of freedom, one in the macrocyclic framework and one in each 9,10-A moiety. When compounds **7c$_n$** are regarded as linkages consisting of $3n$ links and $3n$ joints, the degrees of freedom are calculated as $n - 3$, namely, **7c$_2$**, **7c$_3$**, and **7c$_4$** have 3, 6, and 9 mobilities, respectively.

In order to investigate the dynamic behavior of the cyclic oligomers in solution, we observed the ^{1}H NMR spectra of **6b$_2$** and **7a$_2$** at variable temperatures. We could not measure the spectra of the other compounds at low temperatures because of their low solubility or stability in solution. The signals of **7a$_2$** were sharp and symmetric at room temperature, and became broad at −40 °C and lower temperatures in CD_2Cl_2. The lineshape changes were attributed to the restricted rotation of the butyl groups because similar phenomena were also observed for other cyclic oligomers with alkyl chains at the 10 position.[2,3,9] Hence, the dynamic symmetry of **7a$_2$** is practically D_2 on the NMR time scale contrary to its X-ray and calculated structures of C_2 symmetry. This means that the interconversion between the C_2 structure and its enantiomeric form by skeletal swinging takes place rapidly in solution. The dynamic symmetry of **7a$_3$** (D_3) is also different from the X-ray structure. The molecules should undergo facile exchanges

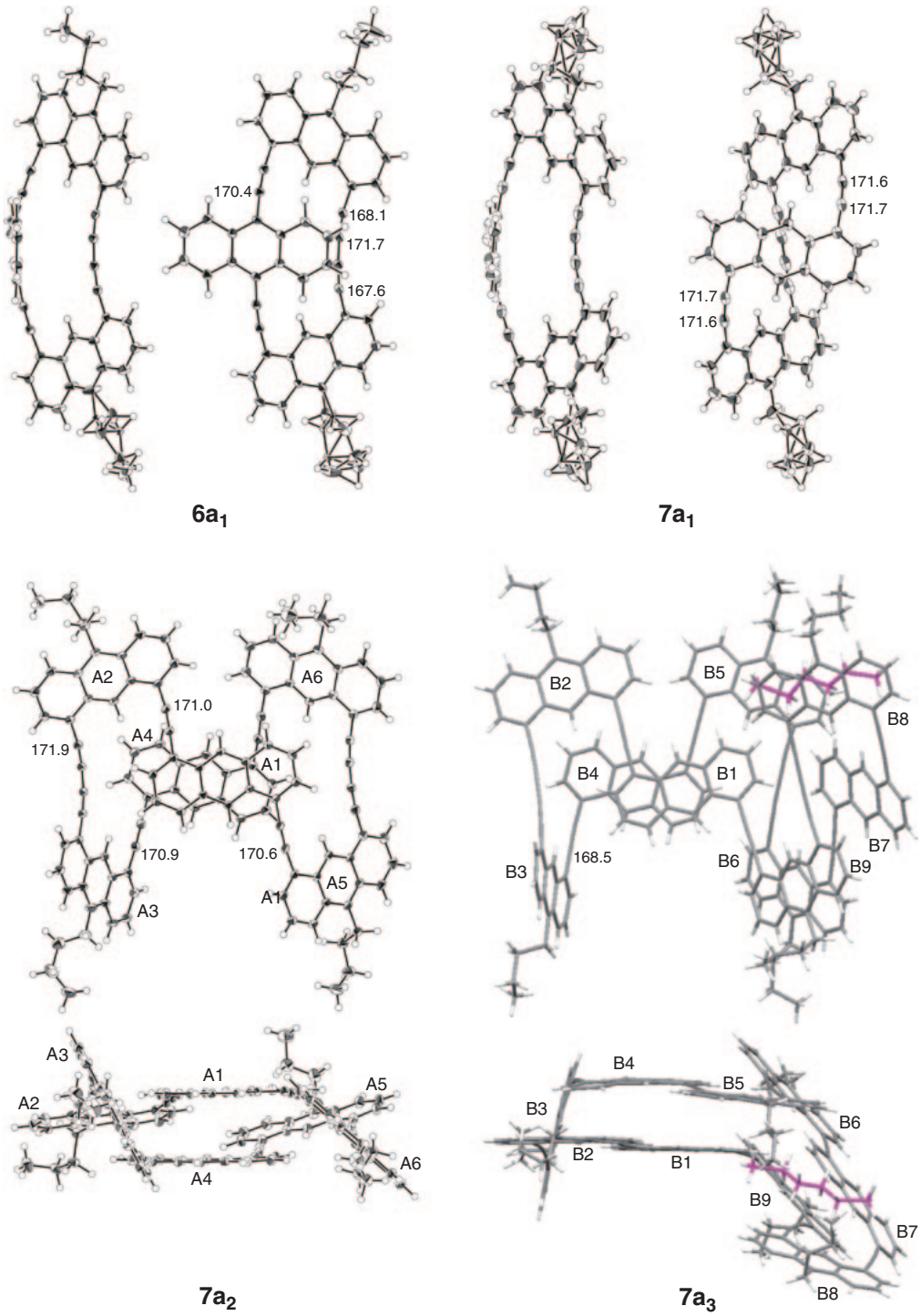

Figure 3. Two views of X-ray structures of **6a**$_1$, **7a**$_1$, **7a**$_2$, and **7a**$_3$. Solvent molecules are omitted for clarity except for **7a**$_3$, where the carbon chain of the included hexane molecule is shown in magenta. Bond angles (°) at alkyne carbons are indicated in the case the angle is smaller than 172°.

between several possible folded conformations in solution even at low temperature. Similar dynamic processes should occur for dodecamer **7a**$_4$ at least at room temperature, although we could not measure its NMR spectra at low temperature. Such motion is regarded as the rolling of a caterpillar belt.

The NMR spectra of **6b**$_2$ were measured in $CDCl_3$ (Figure 5). The lineshape change was observed only for the signals due to the protons in 9,10-A unit. The signal due to H-2,3,6,7 (H-2) at δ 7.5 was observed as a sharp multiplet at 50 °C. This signal broadened at lower temperature and separated into two broad peaks at δ 6.9 and 8.1 at −50 °C. The other signal due to H-1,4,5,8 (H-1) at δ 8.3 was broad at that temperature. This observation is explained by the rotation of the 9,10-A unit about the acetylene axes in the macrocyclic framework, which resulted in an exchange between ABCD and DCBA systems, as shown in Scheme 2. In **6b**$_2$, H_B and H_C are

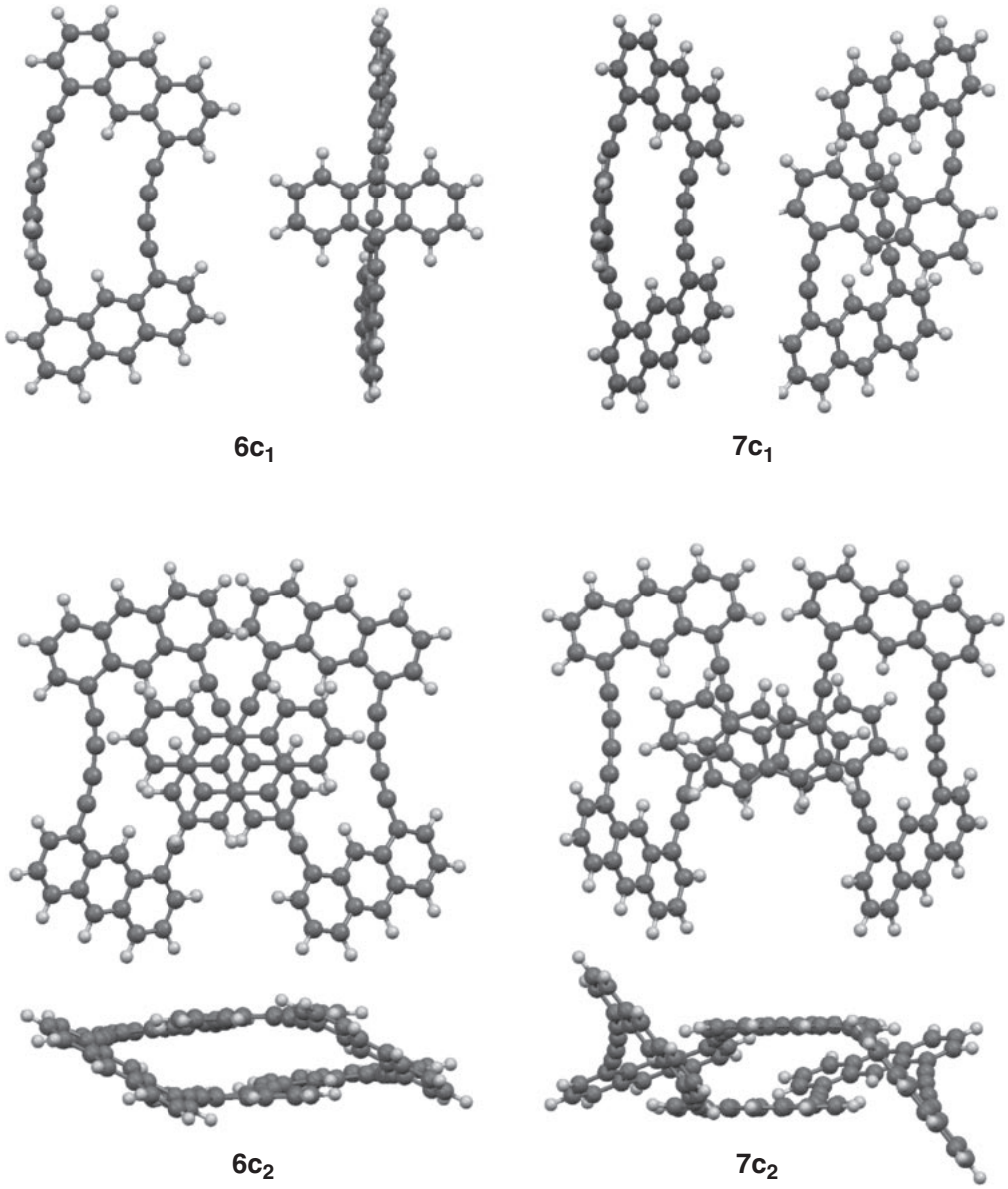

Figure 4. Two views of calculated structures of cyclic trimers, **6c$_1$** and **7c$_1$**, and hexamers, **6c$_2$** and **7c$_2$**, at M05/3-21G level.

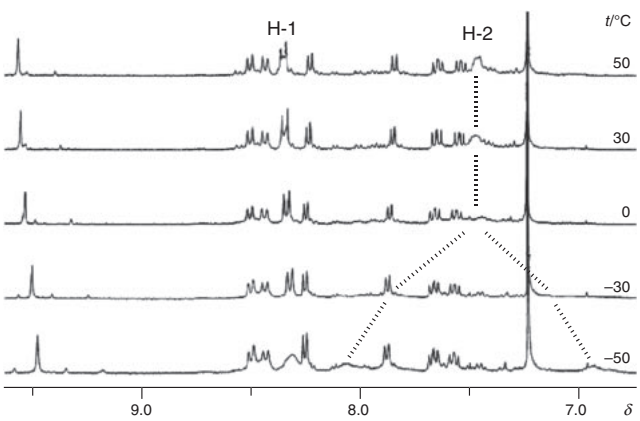

Figure 5. Variable-temperature ^{1}H NMR spectra of **6b$_2$** in $CDCl_3$.

located in the deshielding region of the diyne linker and the shielding region of the 1,8-A unit, respectively, leading to a large difference in the chemical shift. Although the dynamic process was not completely frozen at −51 °C, we estimated the rotational barrier from the coalescence temperature and the chemical shift difference to be 45 kJ mol^{-1} at −30 °C.[21] This barrier is very high for ordinary alkynes, for example the rotational barrier is only 1.4 kJ mol^{-1} for 9,10-bis(phenylethynyl)anthracene.[22,23] In the rotation process in **6b$_2$**, the original state is stabilized by attractive interactions between 9,10-A units as found in the folded form of tetramer **1**.[2] The importance of these interactions is supported by a theoretical study that predicted a large binding energy of the anthracene dimer.[24] Moreover, the transition state should suffer from a large steric hindrance where one of the flanking sides of the 9,10-A units rotates into the inner area of the macrocyclic framework to raise the rotational barrier.

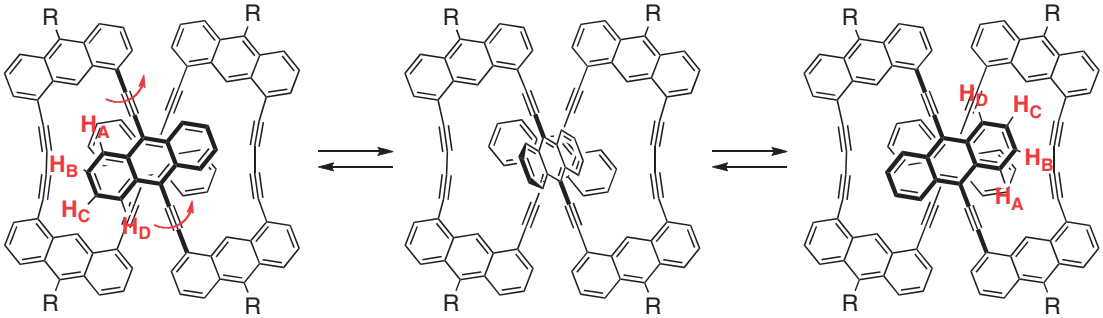

Scheme 2. Rotation of 9,10-A unit about acetylene axes in **6b$_2$** (R = octyl).

Table 2. Enantiomeric Resolution of Chiral Cyclic Oligomers and Their Specific Rotations

	Column[a)]	Easily eluted enantiomer		Less easily eluted enantiomer	
		t_R/min[b)]	$[\alpha]_D$	t_R/min[b)]	$[\alpha]_D$
6b$_2$	IA	48.0	−1120	54.0	+1100
7a$_1$	IC	30.9	+125	42.3	−125
7a$_2$	IC	27.4	−630	30.5	+670
7a$_3$	IC	32.5	+50[c)]	36.5	−44[c)]

a) Daicel CHIRALPAK® IA or CHIRALPAK® IC. For the eluent, see Experimental Section. b) Retention times. c) These values are less reliable because partial decomposition occurred.

Enantiomeric Resolution. The enantiomers of **6b$_2$** and **7a$_1$**–**7a$_3$** could be resolved by chiral HPLC with Daicel CHIRALPAK® I series columns, which are able to tolerate a broad range of solvents.[25] The enantiomers of **6b$_2$** were eluted at 48.0 and 54.0 min with baseline separation when an IA column and hexane/chloroform 3:1 eluent were used. As for the resolution of oligomers **7a$_n$**, an IC column afforded better results than the IA column and the two peaks were well separated under the optimized conditions. The specific rotation (Table 2) and the CD spectra (Figure 6) of the thus resolved enantiomers were measured in chloroform. The absolute values of the specific rotation of **6b$_2$** were very large, −1120 and +1100, in the order of elution. The easily and less easily eluted enantiomers were (−)- and (+)-isomers, respectively, for **6b$_2$** and **7a$_2$**, and vice versa for **7a$_1$** and **7a$_3$**. The CD curves of the enantiomers are mirror images of each other for all the resolved samples. A sample of (−)-**6b$_2$** showed an intense trough at 258 nm, an intense peak at 278 nm, and other weak troughs and peaks in the longer wavelength region. Enantiopure samples of **7a$_1$**–**7a$_3$** gave complicated Cotton effects in the range of 250–480 nm. The Cotton effects of the (−)-isomers at the longest wavelength at ca. 460 nm are plus for **7a$_1$** and **7a$_3$**, and minus for **7a$_2$**. Meanwhile, those of the less easily eluted enantiomers are all minus for the three compounds. From available data, the relationship of the absolute stereochemistry with the chiroptical properties or the chiral recognition of the stationary phase is not always clear. The enantiomeric resolution of **7a$_4$** was unsuccessful because of low solubility and stability.

Then, we attempted the racemization of enantiopure samples of **6b$_2$**, **7a$_1$**, and **7a$_2$** in octane. No racemization was observed at 90–100 °C for several days for all the compounds. The samples significantly decomposed on heating at higher temperature or for longer times. Therefore, we could estimate only the lower limit of the barrier to racemization from heating conditions to be ca. 130 kJ mol^{-1}. This value is higher than that for cyclic tetramer **3** determined by classical kinetics (114 kJ mol^{-1}).[3] These results mean that the chiral macrocyclic structures are enantiomerically very stable because of destabilization of the transition state of the racemization process. The racemization of **7a$_1$** requires the rotation of the 1,5-A moiety about the acetylene axes, during which one of the flanking sides of the anthracene moiety must be directed inside the central ring with severe steric strain. For the racemization of hexamers **6b$_2$** and **7a$_2$**, all anthracene units must turn inside out in the macrocyclic belt. Such process would be possible only with highly strained structures, such as a planar expanded form, although it is not straightforward to predict the actual transition state from available data.

Conclusion

In summary, we successfully obtained macrocyclic oligomers consisting of 3, 6, 9, and 12 anthracene units by the metal-catalyzed cyclization of trimeric precursors. Spectroscopic analyses and DFT calculations revealed that higher oligomers adopted folded structures mainly due to intramolecular $\pi\cdots\pi$ interactions, where the framework was rather rigid for the hexamers and fluxional for the nonamer and the dodecamer. The resolution of such macrocyclic hydrocarbons by chiral HPLC is noteworthy to investigate the chiroptical properties of chiral π-conjugated hydrocarbons. The control of the shape and mobility of belt-shaped molecules is a key issue in the design of functional molecules. The nonamer and the dodecamer in this article give a clue to realize such a possibility, and further studies of the association with or inclusion of foreign materials and the synthesis of larger soluble and stable oligomers are in progress.

Experimental

General. Melting points are uncorrected. NMR spectra were measured on a JEOL GSX-400 (^{1}H: 400 MHz, ^{13}C: 100 MHz) or a JEOL Lambda 500 (^{1}H: 500 MHz, ^{13}C: 125 MHz) spectrometer. High-resolution mass spectra were measured on a JEOL MStation-700 spectrometer by FAB. Elemental analyses were performed with a Perkin-Elmer 2400 series analyzer. UV spectra were measured on a Hitachi U-3000 spectrometer with a 10 mm cell. Fluorescence spectra were measured on a JASCO FP-6500 spectrofluorometer with a 10 mm cell with a sample degassed by Ar gas immediately before measurements.

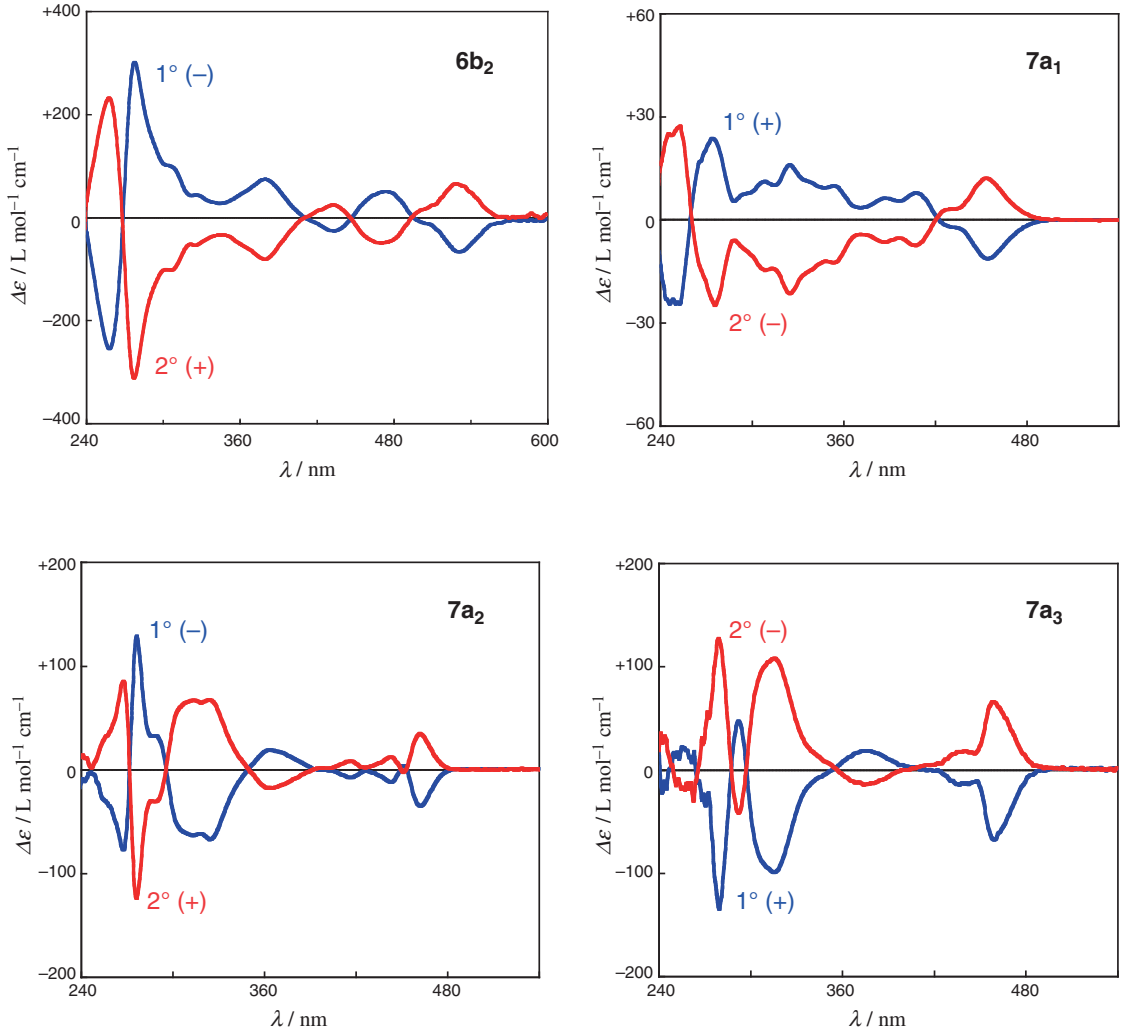

Figure 6. CD spectra of **6b$_2$** and **7a$_1$**–**7a$_3$** in $CHCl_3$. Blue and red curves show spectra for the easily eluted isomer (1°) and the less easily eluted isomers (2°), respectively. Signs of the specific rotation are indicated in parentheses.

The absolute fluorescence quantum yields were recorded on a Hamamatsu photonics C9920-02. The fluorescence lifetimes were measured on a Spectra-Physics time-resolved spectrofluorometer system (Tsunami 3960/50-M2S) with a Ti:Sapphire laser. Optical rotations were measured on a JASCO DIP-370 digital polarimeter with a 3.5 mmϕ × 100 mm cell. CD spectra were measured on a JASCO J-820 polarimeter with a 10 mm cylindrical cell. GPC was performed on a Japan Analytical Industry Co. LC-908 recycling preparative HPLC system with 20 mmϕ × 600 mm JAIGEL-1H, 2H columns using chloroform as eluent. Column chromatography was carried out with Merck Silica Gel 60 (70–230 mesh) or Fuji Silysia Chromatorex-NH (100–200 mesh). The elemental analyses of some oligomers were very difficult because of incomplete combustion, and in such cases the compounds were characterized by HRMS and their purity was confirmed by NMR spectra. Because higher oligomers gave no molecular ion peaks in HRMS spectra, their molecular weights were confirmed by MALDI-TOF spectra including isotope pattern simulation.

Trimer 4b. A solution of **8b**[1] (265 mg, 0.54 mmol) and 9,10-diiodoanthracene (**9**)[11] (116 mg, 0.27 mmol) in a mixture of triethylamine (27 mL) and THF (27 mL) was degassed with Ar gas for 1 h. To the solution were added $[Pd(PPh_3)_4]$ (63 mg, 0.054 mmol) and CuI (10 mg, 0.054 mmol). After the solution was refluxed for 48 h under Ar, the solvent was removed by evaporation. The crude product was purified by chromatography on silica gel with hexane/chloroform (9:1–4:1) eluent to give the desired product as a yellow solid. An analytical sample was obtained by recrystallization from chloroform/methanol. Yield 242 mg (77%); mp 208–210 °C; ^{1}H NMR ($CDCl_3$, 500 MHz): δ 0.47 (6H, m), 0.65 (36H, d, $J = 7.6$ Hz), 0.91 (6H, t, $J = 7.3$ Hz), 1.32–1.38 (4H, m), 1.41–1.45 (12H, m), 1.57–1.63 (4H, m), 1.81–1.88 (4H, m), 3.66 (4H, t, $J = 7.9$ Hz), 7.48 (2H, dd, $J = 7.1$, 9.0 Hz), 7.57–7.62 (6H, m), 7.76 (2H, d, $J = 6.4$ Hz), 8.02 (2H, d, $J = 6.1$ Hz), 8.30 (2H, d, $J = 9.2$ Hz), 8.39 (2H, d, $J = 8.9$ Hz), 8.79 (4H, m), 9.67 (2H, s); ^{13}C NMR ($CDCl_3$, 125 MHz): δ 11.08, 14.10, 18.28, 22.69, 28.40, 29.40, 29.58, 30.31, 31.73, 31.91, 91.29, 97.05, 100.24, 104.90, 118.91, 122.47, 122.71, 123.17, 125.00, 125.03, 125.26, 125.77, 126.89, 127.57, 129.46, 130.99, 131.45, 131.49, 131.59, 132.49, 136.94 (one aromatic signal missing); UV ($CHCl_3$): λ_{max} (ε) 267 (175000), 443 nm (34000); FL ($CHCl_3$): λ_{max} 522 nm (λ_{ex} 393 nm), Φ_f 0.82, τ_f 2.7 ns; HRMS (FAB):

calcd for $C_{84}H_{98}Si_2$ m/z 1162.7207, found m/z 1162.7228 $[M]^+$; Anal. Calcd for $C_{84}H_{98}Si_2$: C, 86.69; H, 8.49%. Found: C, 86.33; H, 8.37%.

Trimer 5a. This compound was similarly prepared from **8a**[2] (185 mg, 0.42 mmol) and 1,5-diiodoanthracene (**10**)[12] (91 mg, 0.21 mmol). The crude product was purified by chromatography on silica gel with hexane/chloroform (9:1–4:1) eluent to give the desired product as a yellow solid. Yield 185 mg (84%); mp 256–258 °C; ^{1}H NMR ($CDCl_3$, 500 MHz): δ 0.67–0.81 (42H, m), 1.06 (6H, t, $J = 7.4$ Hz), 1.63 (4H, sextet, $J = 7.4$ Hz), 1.83 (4H, quintet, $J = 8.0$ Hz), 3.66 (4H, t, $J = 8.0$ Hz), 7.46–7.49 (4H, m), 7.59 (2H, dd, $J = 6.5$, 8.5 Hz), 7.77 (2H, d, $J = 6.7$ Hz), 7.90 (2H, d, $J = 6.4$ Hz), 8.01 (2H, d, $J = 6.8$ Hz), 8.09 (2H, d, $J = 8.5$ Hz), 8.31 (2H, d, $J = 9.2$ Hz), 8.37 (2H, d, $J = 9.2$ Hz), 9.12 (2H, s), 9.62 (2H, s); ^{13}C NMR ($CDCl_3$, 125 MHz): δ 11.13, 14.06, 18.36, 23.34, 28.14, 33.78, 92.61, 92.91, 96.83, 105.11, 121.21, 122.49, 122.61, 123.09, 124.95, 124.98, 125.01, 125.30, 125.61, 126.03, 129.41, 129.43, 129.83, 130.76, 131.15, 131.40, 131.48, 131.50, 131.61, 131.84, 136.82; UV ($CHCl_3$): λ_{max} (ε) 268 (152000), 383 (12800), 404 (24000), 428 nm (30000); FL ($CHCl_3$): λ_{max} 458 nm (λ_{ex} 393 nm), Φ_f 0.64, τ_f 2.7 ns; HRMS (FAB): calcd for $C_{76}H_{82}Si_2$ m/z 1050.5927, found m/z 1050.5955 $[M]^+$; Anal. Calcd for $C_{76}H_{82}Si_2$: C, 86.80; H, 7.86%. Found: C, 86.70; H, 8.14%.

Cyclization of 4b. To a solution of **4b** (100 mg, 0.086 mmol) in THF (23 mL) was added a TBAF solution (0.172 mL of 1.0 mol L^{-1} THF solution, 0.172 mmol). The reaction mixture was stirred at room temperature for 20 min, and the solvent was evaporated. For preparative purpose, this residue was used for the next coupling reaction. An analytical sample was obtained by recrystallization from hexane/chloroform. Desilylated product of **4b**: red solid, mp 212–213 °C; ^{1}H NMR ($CDCl_3$, 500 MHz): δ 0.91 (6H, t, $J = 7.1$ Hz), 1.30–1.37 (12H, m), 1.43 (4H, quintet, $J = 8.0$ Hz), 1.60 (4H, quintet, $J = 7.3$ Hz), 1.84 (4H, quintet, $J = 7.7$ Hz), 3.36 (2H, s), 3.65 (4H, t, $J = 8.3$ Hz), 7.52 (2H, dd, $J = 7.1$, 9.2 Hz), 7.62 (2H, dd, $J = 6.7$, 8.9 Hz), 7.73–7.75 (4H, m), 7.82 (2H, d, $J = 6.7$ Hz), 8.11 (2H, d, $J = 6.5$ Hz), 8.35 (2H, d, $J = 9.2$ Hz), 8.36 (2H, d, $J = 9.2$ Hz), 9.01–9.03 (4H, m), 9.83 (2H, s); ^{13}C NMR ($CDCl_3$, 125 MHz): δ 14.13, 22.66, 28.40, 29.35, 29.56, 30.34, 31.74, 31.92, 82.17, 83.31, 92.25, 101.41, 118.94, 121.23, 122.58, 122.95, 124.94, 125.25, 125.81, 125.91, 127.01, 127.90, 129.38, 129.53, 130.82, 131.12, 131.43, 131.72, 132.35, 137.19; HRMS (FAB): calcd for $C_{66}H_{58}$ m/z 850.4539, found m/z 850.4499 $[M]^+$. To a solution of the terminal alkyne in pyridine (86 mL) was added CuCl (170 mg, 1.72 mmol) and $Cu(OAc)_2 \cdot H_2O$ (427 mg, 2.14 mmol). After the solution was stirred for 22 h at room temperature, the solvent was evaporated. The crude product was subjected to chromatography on silica gel (NH) with hexane/chloroform (9:1) and then with chloroform. The first fraction was practically pure **6b$_1$**. The second fraction was further purified by GPC with chloroform eluent to give **6b$_2$**. Cyclic trimer **6b$_1$**: yellow solid; yield 29 mg (40%); mp 189–190 °C; ^{1}H NMR ($CDCl_3$, 500 MHz): δ 0.91 (6H, t, $J = 6.7$ Hz), 1.31–1.39 (12H, m), 1.44 (4H, quintet, $J = 7.6$ Hz), 1.62 (4H, quintet, $J = 7.9$ Hz), 1.84 (4H, quintet, $J = 7.9$ Hz), 3.63 (4H, quintet, $J = 7.9$ Hz), 7.49 (2H, dd, $J = 7.0$, 8.9 Hz), 7.62–7.67 (6H, m), 7.93 (2H, d, $J = 7.0$ Hz), 7.97 (2H, d, $J = 6.7$ Hz), 8.32 (2H, d, $J = 9.2$ Hz), 8.36 (2H, d, $J = 9.2$ Hz), 8.88–8.90 (4H, m), 9.29 (2H, s); ^{13}C NMR (125 MHz, $CDCl_3$): δ 14.08, 22.66, 28.51, 29.36, 29.56, 30.33, 31.70, 31.90, 80.45, 85.45, 94.49, 101.77, 118.59, 121.97, 121.98, 123.17, 125.15, 125.22, 125.77, 125.99, 127.22, 127.79, 128.14, 129.55, 129.64, 130.56, 132.59, 136.54, 137.38 (one aromatic signal missing); UV ($CHCl_3$): λ_{max} (ε) 261 (127000), 365 (13100), 383 (20600), 491 nm (28400); FL ($CHCl_3$): λ_{max} 541 nm (λ_{ex} 393 nm), Φ_f 0.68, τ_F 3.5 ns; HRMS (FAB): calcd for $C_{66}H_{56}$ m/z 848.4382, found m/z 848.4406 $[M]^+$; Anal. Calcd for $C_{66}H_{56}$: C, 93.35; H, 6.65%. Found: C, 93.18; H, 6.39%. Cyclic hexamer **6b$_2$**: red solid; yield 23 mg (32%); mp 293–296 °C (dec); ^{1}H NMR ($CDCl_3$, 500 MHz): δ 0.94 (12H, t, $J = 6.8$ Hz), 1.35–1.55 (32H, m), 1.71 (8H, quintet, $J = 6.7$ Hz), 1.97 (8H, quintet, $J = 9.5$ Hz), 3.75 (8H, t, $J = 8.6$ Hz), 7.49 (8H, m), 7.56 (4H, dd, $J = 7.0$, 8.9 Hz), 7.66 (4H, dd, $J = 7.1$, 8.9 Hz), 7.86 (4H, d, $J = 6.1$ Hz), 8.24 (4H, d, $J = 6.8$ Hz), 8.33 (8H, m), 8.42 (4H, d, $J = 8.9$ Hz), 8.49 (4H, d, $J = 9.2$ Hz), 9.51 (4H, s); ^{13}C NMR ($CDCl_3$, 125 MHz): δ 14.18, 22.74, 29.43, 29.63, 29.70, 30.50, 31.74, 31.97, 81.14, 85.13, 93.53, 101.11, 117.90, 121.39, 123.06, 123.20, 125.16, 125.20, 125.53, 126.55, 126.59, 127.35, 129.52, 129.81, 130.64, 131.08, 131.17, 132.08, 136.13, 137.50; UV ($CHCl_3$): λ_{max} (ε) 269 (168000), 452 (35600), 487 (37500), 523 nm (33800); FL ($CHCl_3$): λ_{max} 564 nm (λ_{ex} 393 nm), Φ_f 0.69, τ_f 4.5 ns; HRMS (FAB): calcd for $C_{132}H_{112}$ m/z 1696.8764, found m/z 1696.8807 $[M]^+$; Anal. Calcd for $C_{132}H_{112}$: C, 93.35; H, 6.65%. Found: C, 93.45; H, 6.72%.

Cyclization of 4a. The reaction was similarly carried out with **4a**[3] (65 mg, 0.062 mmol). The crude product was purified by chromatography on silica gel (NH) with hexane/chloroform 9:1 eluent. Cyclic trimer **6a$_1$**: yellow solid; yield 17 mg (37%); mp 327–328 °C; ^{1}H NMR ($CDCl_3$, 300 MHz): δ 1.06 (6H, t, $J = 7.8$ Hz), 1.64 (4H, sextet, $J = 6.9$ Hz), 1.83 (4H, quintet, $J = 7.2$ Hz), 3.64 (4H, t, $J = 7.8$ Hz), 7.49 (2H, dd, $J = 7.2$, 8.7 Hz), 7.60–7.68 (6H, m), 7.92 (2H, d, $J = 6.9$ Hz), 7.96 (2H, d, $J = 6.9$ Hz), 8.26–8.36 (4H, m), 8.87–8.91 (4H, m), 9.28 (2H, s); ^{13}C NMR ($CDCl_3$, 125 MHz): δ 14.08, 23.43, 28.22, 33.79, 80.41, 85.47, 94.47, 101.73, 118.58, 121.94, 123.16, 125.18, 125.24, 125.78, 126.01, 127.24, 127.79, 128.16, 129.54, 129.64, 130.53, 132.58, 136.67, 137.33 (two aromatic signals missing); UV ($CHCl_3$): λ_{max} (ε) 261 (190000), 366 (20100), 383 (31800), 491 nm (44300); FL ($CHCl_3$): λ_{max} 541 nm (λ_{ex} 393 nm), HRMS (FAB): calcd for $C_{58}H_{40}$ m/z 736.3130, found m/z 736.3131 $[M]^+$. Cyclic hexamer **6a$_2$**: red solid; yield 9 mg (20%); mp 342–343 °C; ^{1}H NMR ($CDCl_3$, 400 MHz, 50 °C): δ 1.15 (12H, t, $J = 7.2$ Hz), 1.73 (8H, sextet, $J = 6.8$ Hz), 1.98 (8H, quintet, $J = 8.4$ Hz), 3.77 (8H, t, $J = 7.2$ Hz), 7.47 (8H, m), 7.54 (4H, dd, $J = 6.8$, 9.2 Hz), 7.65 (4H, dd, $J = 7.2$, 8.8 Hz), 7.84 (4H, d, $J = 6.8$ Hz), 8.22 (4H, d, $J = 6.0$ Hz), 8.35 (8H, m), 8.42 (4H, d, $J = 8.8$ Hz), 8.49 (4H, d, $J = 8.8$ Hz), 9.53 (4H, s); UV ($CHCl_3$): λ_{max} (ε) 270 (91600), 491 (22200), 525 nm (22400); FL ($CHCl_3$); λ_{max} 565 nm (λ_{ex} 393 nm); MALDI-TOFMS: calcd for $C_{116}H_{80}$ m/z 1472.82, found: m/z 1472.63 $[M]^+$.

Cyclization of 5a. The reaction was similarly carried out with **5a** (94 mg, 0.089 mmol). Desilylated product of **5a**: orange solid; mp 276–279 °C (dec); ^{1}H NMR ($CDCl_3$,

500 MHz): δ 1.06 (6H, t, $J = 7.1$ Hz), 1.63 (4H, sextet, $J = 7.0$ Hz), 1.84 (4H, quintet, $J = 8.3$ Hz), 3.19 (2H, s), 3.66 (4H, t, $J = 8.6$ Hz), 7.51 (2H, dd, $J = 7.1$, 8.9 Hz), 7.56–7.62 (4H, m), 7.81 (2H, d, $J = 6.7$ Hz), 8.01 (2H, d, $J = 7.0$ Hz), 8.03 (2H, d, $J = 6.7$ Hz), 8.24 (2H, d, $J = 8.6$ Hz), 8.35–8.37 (4H, m), 9.36 (2H, s), 9.84 (2H, s); ^{13}C NMR (125 MHz, $CDCl_3$): δ 14.07, 23.37, 28.07, 33.82, 81.97, 83.21, 93.42, 93.48, 121.23, 121.31, 122.43, 122.96, 124.90, 125.23, 125.58, 125.93, 126.37, 129.33, 129.52, 130.15, 130.41, 131.05, 131.09, 131.39, 131.55, 131.63, 131.71, 137.03 (one aromatic signal missing); HRMS (FAB): calcd for $C_{58}H_{42}$ m/z 738.3287, found: m/z 738.3333 $[M]^+$. After cyclization, the crude product was subjected to chromatography on silica gel (NH) with hexane/chloroform (9:1) and then with chloroform. The first fraction was recrystallized from *m*-xylene/ethanol to give pure **7a$_1$**. The second fraction was further purified by GPC with chloroform, and separated into three products **7a$_2$**–**7a$_4$**. Cyclic trimer **7a$_1$**: yellow crystals; yield 1.9 mg (3%); mp 255–256 °C; ^{1}H NMR (500 MHz, $CDCl_3$): δ 1.08 (6H, t, $J = 7.3$ Hz), 1.66 (4H, sextet, $J = 7.3$ Hz), 1.87 (4H, quintet, $J = 7.3$ Hz), 3.66 (4H, t, $J = 7.3$ Hz), 7.24–7.29 (2H, m), 7.40 (2H, dd, $J = 7.0$, 8.6 Hz), 7.54–7.63 (6H, m), 7.80 (2H, d, $J = 6.8$ Hz), 7.86 (2H, d, $J = 6.4$ Hz), 8.30 (2H, d, $J = 8.9$ Hz), 8.36 (2H, d, $J = 8.9$ Hz), 9.29 (2H, s), 9.58 (2H, s); UV ($CHCl_3$): λ_{max} (ε) 269 (141000), 457 nm (34600); FL ($CHCl_3$): λ_{max} 506 nm (λ_{ex} 393 nm), Φ_f 0.50, τ_f 2.7 ns; HRMS (FAB): calcd for $C_{58}H_{40}$ m/z 736.3130, found: m/z 736.3137 $[M]^+$. Cyclic hexamer **7a$_2$**: yellow solid; yield 20 mg (30%); mp 342–343 °C; ^{1}H NMR (500 MHz, $CDCl_3$): δ 1.13 (12H, t, $J = 8.0$ Hz), 1.72 (8H, sextet, $J = 8.0$ Hz), 1.94 (8H, quintet, $J = 7.9$ Hz), 3.73 (8H, t, $J = 8.0$ Hz), 7.09 (4H, dd, $J = 7.0$, 8.6 Hz), 7.43 (4H, d, $J = 8.6$ Hz), 7.56 (4H, dd, $J = 6.8$, 8.9 Hz), 7.62 (4H, dd, $J = 6.7$, 9.2 Hz), 7.79 (4H, d, $J = 6.4$ Hz), 7.81 (4H, d, $J = 6.4$ Hz), 7.89 (4H, d, $J = 6.8$ Hz), 8.38–8.40 (8H, m), 8.43 (4H, d, $J = 8.5$ Hz), 9.79 (4H, s); ^{13}C NMR (125 MHz, $CDCl_3$): δ 14.15, 23.50, 28.20, 33.88, 79.40, 82.46, 93.04, 95.01, 119.82, 121.14, 122.70, 123.24, 124.96, 125.10, 125.14, 125.23, 125.35, 126.43, 128.97, 129.33, 129.62, 129.67, 130.21, 130.53, 130.78, 131.33, 131.88, 133.51, 137.13; UV ($CHCl_3$): λ_{max} (ε) 271 (169000), 437 (37700), 460 nm (41700); FL ($CHCl_3$): λ_{max} 494 nm (λ_{ex} 393 nm), Φ_f 0.49, τ_f 3.7 ns; HRMS (FAB): calcd for $C_{116}H_{80}$ m/z 1472.6260, found: m/z 1472.6249 $[M]^+$; Anal. Calcd for $C_{116}H_{80} + 3C_6H_5Cl$: C, 88.84; H, 5.29%. Found: C, 88.97; H, 5.45%. Cyclic nonamer **7a$_3$**: yellow crystal; yield 10 mg (15%); mp 301–302 °C (dec); ^{1}H NMR (300 MHz, $CDCl_3$): δ 1.09 (18H, t, $J = 6.4$ Hz), 1.62–1.70 (12H, m), 1.84–1.88 (12H, m), 3.59 (12H, m), 7.02 (6H, t, $J = 8.1$ Hz), 7.39–7.44 (18H, m), 7.54 (6H, d, $J = 6.4$ Hz), 7.67 (6H, d, $J = 6.1$ Hz), 7.80 (6H, d, $J = 7.9$ Hz), 8.20 (6H, d, $J = 8.0$ Hz), 8.31 (6H, d, $J = 8.0$ Hz), 8.48 (6H, s), 9.44 (6H, s); UV ($CHCl_3$): λ_{max} (ε) 271 (218000), 436 (50700), 463 nm (57300); FL ($CHCl_3$): λ_{max} 485 nm (λ_{ex} 393 nm), Φ_f 0.41, τ_f 3.5 ns; MS (MALDI-TOF): calcd for $^{12}C_{172}{}^{13}C_2H_{120}$ m/z 2210.95, found: m/z 2210.47 $[M]^+$. Cyclic dodecamer **7a$_4$**: yellow solid; yield 9 mg (14%); mp 293–295 °C; ^{1}H NMR (300 MHz, $CDCl_3$): δ 1.09 (24H, t, $J = 6.6$ Hz), 1.53–1.68 (16H, m), 1.85 (16H, m), 3.57–3.63 (16H, m), 6.80 (8H, t, $J = 7.2$ Hz), 7.23–7.30 (16H, m), 7.45 (8H, m), 7.51 (8H, d, $J = 7.5$ Hz), 7.71 (8H, d, $J = 6.6$ Hz), 7.77 (8H, d, $J = 7.5$ Hz), 8.20 (8H, d, $J = 8.4$ Hz), 8.25 (8H, d, $J = 8.4$ Hz), 8.36 (8H, s), 9.38 (8H, s); UV ($CHCl_3$): λ_{max} (ε) 270 (254000), 435 (59400), 463 nm (65800); FL ($CHCl_3$): λ_{max} 506 nm (λ_{ex} 393 nm), Φ_f 0.14, τ_f 1.4, 3.5 ns; HRMS (MALDI-TOF): calcd for $^{12}C_{229}{}^{13}C_3H_{160}$ m/z 2948.26, found: m/z 2948.57 $[M]^+$.

X-ray Analysis. Single crystals used for the measurements were obtained by recrystallization from bromobenzene (**6a$_1$**), *m*-xylene/ethanol (**7a$_1$**), chlorobenzene (**7a$_2$**), and hexane/$CHCl_3$ (**7a$_3$**). Diffraction data were collected on a Rigaku R-AXIS IV (**6a$_1$** and **7a$_1$**), Rigaku FR-E+ SuperBright (**7a$_2$**), or Rigaku VariMax with RAPID (**7a$_3$**). Computations were performed using Yadokari-XG 2009[26] or CrystalStructure crystallographic software.[27] The structure was solved by the direct method (SHELXS-97) and refined by the full-matrix least-squares method (SHELXL-97).[28] Non-hydrogen atoms were refined anisotropically. Hydrogen atoms were refined isotropically, and some of them were refined using the riding model. Additional crystallographic data are as follows. **6a$_1$**: crystal dimension $0.04 \times 0.04 \times 0.02$ mm^3, formula $C_{58}H_{40}\cdot 1/2(C_6H_5Br)$, $M_r = 811.37$, triclinic, space group $P\bar{1}$ (No. 2), $a = 11.2405(8)$, $b = 13.4781(11)$, $c = 15.2195(9)$ Å, $\alpha = 114.188(2)$, $\beta = 90.069(4)$, $\gamma = 90.2529(6)°$, $V = 2103.3(3)$ Å^3, $Z = 2$, $D_{calcd} = 1.281$ g cm^{-3}, μ(Mo Kα) = 0.544 mm^{-1}, $T = 93$ K, $F(000) = 844$, 8863 observed reflections, $R1 = 0.0772$ $[I > 2.00\sigma(I)]$, $wR2 = 0.1848$ (all data), GOF 1.00. **7a$_1$**: crystal dimension $0.25 \times 0.07 \times 0.03$ mm^3, formula $1/2(C_{58}H_{40}\cdot C_8H_{10})$, $M_r = 421.53$, monoclinic, space group $C2/c$ (No. 15), $a = 24.3186(6)$, $b = 13.6845(3)$, $c = 14.4806(3)$ Å, $\beta = 106.9323(16)$, $V = 4610.06(18)$ Å^3, $Z = 8$, $D_{calcd} = 1.215$ g cm^{-3}, μ(Mo Kα) = 0.069 mm^{-1}, $T = 123$ K, $F(000) = 1784$, 5295 observed reflections, $R1 = 0.0853$ $[I > 2.00\sigma(I)]$, $wR2 = 0.1574$ (all data), GOF 1.09. **7a$_2$**: crystal dimension $0.10 \times 0.09 \times 0.02$ mm^3; formula $C_{116}H_{80}\cdot 4(C_6H_5Cl)$, $M_r = 1924.00$; triclinic, space group $P\bar{1}$ (No. 2), $a = 12.6918(4)$, $b = 18.6702(5)$, $c = 22.5712(7)$ Å, $\alpha = 78.3714(15)$, $\beta = 80.143(2)$, $\gamma = 80.4223(11)°$, $V = 5112.9(3)$ Å^3, $Z = 2$, $D_{calcd} = 1.250$ g cm^{-3}, μ(Mo Kα) = 0.172 mm^{-1}, $T = 103$ K, $F(000) = 2016$, 21749 observed reflections, $R1 = 0.0790$ $[I > 2.00\sigma(I)]$, $wR2 = 0.2211$ (all data), GOF 1.01. **7a$_3$**: crystal dimension $0.12 \times 0.11 \times 0.09$ mm^3, formula $C_{180}H_{134}$, $M_r = 2297.04$, monoclinic, space group $P2_1/c$ (No. 14), $a = 27.927(2)$, $b = 24.4485(4)$, $c = 22.2743(4)$ Å, $\beta = 93.881(6)°$, $V = 15174(1)$ Å^3, $Z = 4$, $D_{calcd} = 1.005$ g cm^{-3}, μ(Cu Kα) = 0.429 mm^{-1}, $T = 93$ K, $F(000) = 4856$, 26902 observed reflections, $R1 = 0.0856$ $[I > 2.00\sigma(I)]$, $wR2 = 0.2038$ (all data), GOF 1.213. The included solvent molecules (chloroform and hexane) except for one hexane molecule shown in Figure 3 were highly disordered in the single crystal of **7a$_3$**, and could not be refined in an ordinary manner. These solvent atoms corresponding to 466 electrons in a cavity of 3138 Å^3 were implemented as SQUEEZE procedure in PLATON.[29] Thus treated solvent molecules were not considered in the above parameters. Crystallographic data have been deposited with the Cambridge Crystallographic Data Centre: Deposition numbers CCDC-814932 (**6a$_1$**), -814933 (**7a$_1$**), -814934 (**7a$_2$**), and -814935 (**7a$_3$**). Copies of the data can be obtained free of charge via http://www.ccdc.cam.ac.uk/conts/retrieving.html (or from the Cambridge Crystallographic Data Centre, 12, Union Road, Cam-

bridge, CB2 1EZ, U.K.; Fax: +44 1223 336033; e-mail: deposit@ccdc.cam.ac.uk).

VT ^{1}H NMR Measurement. The ^{1}H NMR spectra of **6b$_2$**, **7a$_2$**, and **7a$_3$** were measured at variable temperatures on the JEOL GSX-400 spectrometer in CD_2Cl_2 or $CDCl_3$. The temperature was read from a thermocouple after calibration with the chemical shift differences of signals of methanol or 1,2-ethanediol. In the spectra of **6b$_2$** measured in $CDCl_3$, the signals due to the H-2,3,6,7 atoms in 9,10-A were observed at δ 6.9 and 8.1 (chemical shift difference 448 Hz) at -50 °C, and coalesced at ca. -30 °C. The rate of exchange at the coalescence temperature was calculated to be $1.0 \times 10^3\,s^{-1}$ from the conventional equation.[30] These values gave the free energy of activation for the site-exchange to be $\Delta G^{\neq}$ 45 kJ mol^{-1} at 243 K.

DFT Calculation. The calculations were carried out with Gaussian 03W[31] on a Windows computer. The structures were optimized by hybrid DFT at the M05/3-21G level from several input structures.

Enantiomeric Resolution. Chiral HPLC of **6b$_2$** and **7a$_1$**–**7a$_3$** was carried out with a Daicel CHIRALPAK® IA or IC column (10 mmϕ × 250 mm). A solution of ca. 0.01–0.15 mg of a racemic sample in the eluent (1 mL) was injected for each batch with flow rate of 0.5 mL min^{-1}. **6b$_2$**: column IA; retention times 48.0, 54.0 min; eluent hexane/chloroform 3:1. Easily eluted isomer: red solid; mp 175–176 °C; $[\alpha]_D^{22}$ −1120 (*c* 0.002, $CHCl_3$); CD ($CHCl_3$): λ ($\Delta\varepsilon$) 258 (−254.6), 278 (+301.1), 380 (+74.5), 434 (−25.6), 473 (+51.0), 531 nm (−66.6). Less easily eluted isomer: red solid; mp 177–178 °C; $[\alpha]_D^{22}$ +1100 (*c* 0.003, $CHCl_3$); CD ($CHCl_3$): λ ($\Delta\varepsilon$) 258 (+231.6), 277 (−311.4), 380 (−80.7), 432 (+25.1), 470 (−49.1), 527 nm (+65.5). **7a$_1$**: column IC; retention times 30.9, 42.3 min; eluent hexane/2-propanol/dichloromethane 50:1:1. Easily eluted isomer: yellow needles; mp 289–290 °C; $[\alpha]_D^{28}$ +125 (*c* 0.013, $CHCl_3$); CD ($CHCl_3$): λ ($\Delta\varepsilon$) 252 (−24.3), 274 (+23.7), 325 (+16.0), 407 (+7.8), 456 nm (−11.1). Less easily eluted isomer: yellow needles; mp 290–291 °C; $[\alpha]_D^{28}$ −125 (*c* 0.010, $CHCl_3$); CD ($CHCl_3$): λ ($\Delta\varepsilon$) 253 (+27.2), 276 (−24.8), 325 (−21.5), 407 (−7.5), 453 nm (+12.2). **7a$_2$**: column IC; retention times 27.4, 30.5 min; eluent hexane/THF 5:1. Easily eluted isomer: yellow solid; mp 313–314 °C; $[\alpha]_D^{22}$ −630 (*c* 0.003, $CHCl_3$); CD ($CHCl_3$): λ ($\Delta\varepsilon$) 268 (−76.7), 276 (+128.4), 313 (−63.1), 324 (−67.0), 363 (+18.9), 417 (−7.2), 443 (−12.0), 462 nm (−34.8). Less easily eluted isomer: yellow solid; mp 312–313 °C; $[\alpha]_D^{22}$ +670 (*c* 0.002, $CHCl_3$); CD ($CHCl_3$): λ ($\Delta\varepsilon$) 268 (+84.8), 276 (−123.7), 314 (+67.2), 324 (+67.4), 365 (−17.6), 417 (+8.4), 443 (+12.2), 462 nm (+34.8). **7a$_3$**: column IC; retention times 32.5, 36.5 min; eluent hexane/THF 5:1. Easily eluted isomer: yellow solid; $[\alpha]_D^{22}$ +50 (*c* 0.030, $CHCl_3$); CD ($CHCl_3$): λ ($\Delta\varepsilon$) 280 (−134.6), 292 (+47.4), 315 (−99.2), 374 (+18.7), 460 nm (−67.8). Less easily eluted isomer: yellow solid; $[\alpha]_D^{22}$ −44 (*c* 0.024, $CHCl_3$); CD ($CHCl_3$): λ ($\Delta\varepsilon$) 280 (+124.6), 292 (−41.8), 316 (+108.0), 374 (−14.2), 459 nm (+66.2). Melting points of the enantiopure samples of **7a$_3$** could not be measured because of the very small quantity and decomposition.

Kinetic Measurement. A solution of (−)-**6b$_2$** (0.1 mg) in dry octane (5 mL) was heated in an oil bath at 90 °C for 72 h. The other enantiomer was not detected by chiral HPLC. The rate constant of racemization should be $k < 2 \times 10^{-7}\,s^{-1}$ (assuming <5% racemization), and this value corresponds to $\Delta G^{\neq} > 128$ kJ mol^{-1}. A solution of (−)-**7a$_2$** (0.5 mg) in dry octane (6 mL) was heated at 90 °C for 114 h, showing no racemization: $k < 1 \times 10^{-7}\,s^{-1}$, $\Delta G^{\neq} > 130$ kJ mol^{-1}. A solution of (+)-**7a$_1$** (0.5 mg) in octane (6 mL) was heated at 100 °C for 96 h, showing no racemization: $k < 1.5 \times 10^{-7}\,s^{-1}$, $\Delta G^{\neq} > 141$ kJ mol^{-1}. When the above solutions were heated at higher temperature, the samples decomposed within a few hours without racemization. An experiment with compound **7a$_3$** was unsuccessful because of facile decomposition in boiling chloroform.

This work was partly supported by Grants-in-Aid for Scientific Research (C) No. 19550054 and for Scientific Research on Innovative Areas (Integrated Organic Synthesis) No. 22106543 from MEXT (Ministry of Education, Culture, Sports, Science and Technology, Japan) and by a matching fund subsidy for private universities from MEXT. The authors thank Associate Professor K. Wakamatsu for valuable discussion in computational chemistry. A part of this manuscript was prepared at Institute for Materials Chemistry and Engineering, Kyushu University, where one of the authors (ST) had been appointed as visiting professor. The helpful support of Professor T. Shinmyozu of the institute is also acknowledged.

References

1 Part 17 of the series "Chemistry of Anthracene–Acetylene Oligomers:" S. Toyota, T. Kawakami, R. Shinnishi, R. Sugiki, S. Suzuki, T. Iwanaga, *Org. Biomol. Chem.* **2010**, *8*, 4997.

2 a) S. Toyota, M. Goichi, M. Kotani, *Angew. Chem., Int. Ed.* **2004**, *43*, 2248. b) S. Toyota, M. Goichi, M. Kotani, M. Takezaki, *Bull. Chem. Soc. Jpn.* **2005**, *78*, 2214.

3 a) T. Ishikawa, T. Shimasaki, H. Akashi, S. Toyota, *Org. Lett.* **2008**, *10*, 417. b) T. Ishikawa, T. Shimasaki, H. Akashi, T. Iwanaga, S. Toyota, M. Yamasaki, *Bull. Chem. Soc. Jpn.* **2010**, *83*, 220.

4 a) V. Haridas, H. Singh, Y. K. Sharma, K. Lal, *J. Chem. Sci.* **2007**, *119*, 219. b) K. Tahara, Y. Tobe, *Chem. Rev.* **2006**, *106*, 5274. c) T. Kawase, H. Kurata, *Chem. Rev.* **2006**, *106*, 5250. d) T. Kawase, *Synlett* **2007**, 2609. e) R. Herges, *Chem. Rev.* **2006**, *106*, 4820. f) R. Gleiter, B. Hellbach, S. Gath, R. J. Schaller, *Pure Appl. Chem.* **2006**, *78*, 699. g) P. Kissel, J. van Heijst, R. Enning, A. Stemmer, A. D. Schlüter, J. Sakamoto, *Org. Lett.* **2010**, *12*, 2778. h) K. Miki, M. Fujita, Y. Inoue, Y. Senda, T. Kowada, K. Ohe, *J. Org. Chem.* **2010**, *75*, 3537.

5 a) J.-Y. Shin, H. Furuta, K. Yoza, S. Igarashi, A. Osuka, *J. Am. Chem. Soc.* **2001**, *123*, 7190. b) J. M. Lim, J.-Y. Shin, Y. Tanaka, S. Saito, A. Osuka, D. Kim, *J. Am. Chem. Soc.* **2010**, *132*, 3105. c) S. Saito, K. Furukawa, A. Osuka, *J. Am. Chem. Soc.* **2010**, *132*, 2128. d) C. Bucher, D. Seidel, V. Lynch, J. L. Sessler, *Chem. Commun.* **2002**, 328. e) H. Rath, J. Sankar, V. PrabhuRaja, T. K. Chandrashekar, B. S. Joshi, R. Roy, *Chem. Commun.* **2005**, 3343.

6 K. Yano, M. Osatani, K. Tani, T. Adachi, K. Yamamoto, H. Matsubara, *Bull. Chem. Soc. Jpn.* **2000**, *73*, 185.

7 a) R. Gleiter, B. Esser, S. C. Kornmayer, *Acc. Chem. Res.* **2009**, *42*, 1108. b) B. Esser, F. Rominger, R. Gleiter, *J. Am. Chem. Soc.* **2008**, *130*, 6716.

8 a) R. Jasti, J. Bhattacharjee, J. B. Neaton, C. R. Bertozzi, *J. Am. Chem. Soc.* **2008**, *130*, 17646. b) H. Takaba, H. Omachi, Y.

Yamamoto, J. Bouffard, K. Itami, *Angew. Chem., Int. Ed.* **2009**, *48*, 6112. c) S. Yamago, Y. Watanabe, T. Iwamoto, *Angew. Chem., Int. Ed.* **2010**, *49*, 757.

9 a) S. Toyota, S. Suzuki, M. Goichi, *Chem.—Eur. J.* **2006**, *12*, 2482. b) S. Toyota, H. Onishi, K. Wakamatsu, T. Iwanaga, *Chem. Lett.* **2009**, *38*, 350. c) S. Toyota, H. Miyahara, M. Goichi, S. Yamasaki, T. Iwanaga, *Bull. Chem. Soc. Jpn.* **2009**, *82*, 931. d) S. Toyota, *Chem. Lett.* **2011**, *40*, 12.

10 a) S. Kammermeier, P. G. Jones, R. Herges, *Angew. Chem., Int. Ed. Engl.* **1996**, *35*, 2669. b) S. Kammermeier, P. G. Jones, R. Herges, *Angew. Chem., Int. Ed. Engl.* **1997**, *36*, 2200. c) R. Herges, M. Deichmann, T. Wakita, Y. Okamoto, *Angew. Chem., Int. Ed.* **2003**, *42*, 1170.

11 B. F. Duerr, Y. S. Chung, A. W. Czarnik, *J. Org. Chem.* **1988**, *53*, 2120.

12 J. K. Kendall, H. Shechter, *J. Org. Chem.* **2001**, *66*, 6643.

13 a) P. Siemsen, R. C. Livingston, F. Diederich, *Angew. Chem., Int. Ed.* **2000**, *39*, 2632. b) J. A. Marsden, J. J. Miller, L. D. Shirtcliff, M. M. Haley, *J. Am. Chem. Soc.* **2005**, *127*, 2464.

14 G. Gleiter, R. Merger, in *Modern Acetylene Chemistry*, ed. by P. J. Stang, F. Diederich, VCH, Weinheim, **1995**, Chap. 8.

15 a) S. Akiyama, K. Nakasuji, M. Nakagawa, *Bull. Chem. Soc. Jpn.* **1971**, *44*, 2231. b) S. Akiyama, K. Nakashima, S. Nakatsuji, M. Nakagawa, *Dyes Pigm.* **1990**, *13*, 117. c) L. Flamigni, A. M. Talarico, B. Ventura, R. Rein, N. Solladié, *Chem.—Eur. J.* **2006**, *12*, 701.

16 a) U. H. F. Bunz, *Chem. Rev.* **2000**, *100*, 1605. b) I.-B. Kim, R. Phillips, U. H. F. Bunz, *Macromolecules* **2007**, *40*, 5290.

17 a) B. Valeur, *Molecular Fluorescence: Principles and Applications*, Wiley-VCH, Weinheim, **2002**, Chap. 4. b) J. R. Lakowicz, *Principles of Fluorescence Spectroscopy*, 3rd ed., Springer, New York, **2006**, Chap. 8.

18 Y. Zhao, D. G. Truhlar, *Acc. Chem. Res.* **2008**, *41*, 157.

19 The calculations of higher cyclic oligomers of **7c$_3$** were possible by a semiempirical method (AM1 and PM3) and molecular mechanics. However, those methods could not reproduce the observed folded structures at all because of the underestimation of attractive $\pi\cdots\pi$ interactions.

20 In the field of mechanical engineering, the degrees of freedom of linkages can be calculated by the Kutzbach–Gruebler's equation: $m = 3(n - 1) - 2f$, where m is the degree of freedom, n is the number of links, and f is the number of linkers of one degree of freedom.

21 Unfortunately, we could not measure the ^{1}H NMR spectra at lower temperature in other solvents with low melting points. For example, the sample decomposed significantly in CD_2Cl_2.

22 S. Toyota, *Chem. Rev.* **2010**, *110*, 5398.

23 a) A. Beeby, K. S. Findlay, A. E. Goeta, L. Porrès, S. R. Rutter, A. L. Thompson, *Photochem. Photobiol. Sci.* **2007**, *6*, 982. b) M. Levitus, M. A. Garcia-Garibay, *J. Phys. Chem. A* **2000**, *104*, 8632.

24 a) C. Gonzalez, E. C. Lim, *J. Phys. Chem. A* **2000**, *104*, 2953. b) C. Gonzalez, E. C. Lim, *J. Phys. Chem. A* **2003**, *107*, 10105. c) R. Podeszwa, K. Szalewicz, *Phys. Chem. Chem. Phys.* **2008**, *10*, 2735. d) S. Chen, Q. Yan, T. Li, D. Zhao, *Org. Lett.* **2010**, *12*, 4784.

25 T. Ikai, Y. Okamoto, *Chem. Rev.* **2009**, *109*, 6077.

26 C. Kabuto, S. Akine, T. Nemoto, E. Kwon, *J. Cryst. Soc. Jpn.* **2009**, *51*, 218.

27 *CrystalStructure 4.0: Crystal Structure Analysis Package*, Rigaku Corporation, Tokyo, **2010**.

28 G. M. Sheldrick, *Acta Crystallogr., Sect. A* **2008**, *64*, 112.

29 A. L. Spek, *Acta Crystallogr., Sect. D* **2009**, *65*, 148.

30 M. Ōki, *Applications of Dynamic NMR Spectroscopy to Organic Chemistry*, VCH, Deerfield Beach, **1985**, Chap. 1.

31 M. J. Frisch, G. W. Trucks, H. B. Schlegel, G. E. Scuseria, M. A. Robb, J. R. Cheeseman, J. A. Montgomery, Jr., T. Vreven, K. N. Kudin, J. C. Burant, J. M. Millam, S. S. Iyengar, J. Tomasi, V. Barone, B. Mennucci, M. Cossi, G. Scalmani, N. Rega, G. A. Petersson, H. Nakatsuji, M. Hada, M. Ehara, K. Toyota, R. Fukuda, J. Hasegawa, M. Ishida, T. Nakajima, Y. Honda, O. Kitao, H. Nakai, M. Klene, X. Li, J. E. Knox, H. P. Hratchian, J. B. Cross, V. Bakken, C. Adamo, J. Jaramillo, R. Gomperts, R. E. Stratmann, O. Yazyev, A. J. Austin, R. Cammi, C. Pomelli, J. W. Ochterski, P. Y. Ayala, K. Morokuma, G. A. Voth, P. Salvador, J. J. Dannenberg, V. G. Zakrzewski, S. Dapprich, A. D. Daniels, M. C. Strain, O. Farkas, D. K. Malick, A. D. Rabuck, K. Raghavachari, J. B. Foresman, J. V. Ortiz, Q. Cui, A. G. Baboul, S. Clifford, J. Cioslowski, B. B. Stefanov, G. Liu, A. Liashenko, P. Piskorz, I. Komaromi, R. L. Martin, D. J. Fox, T. Keith, M. A. Al-Laham, C. Y. Peng, A. Nanayakkara, M. Challacombe, P. M. W. Gill, B. Johnson, W. Chen, M. W. Wong, C. Gonzalez, J. A. Pople, *Gaussian 03 (Revision E.01)*, Gaussian, Inc., Wallingford CT, **2004**.